

Network structure of epoxies – a neutron scattering study: 2.

Wen-li Wu and Barry J. Bauer

Polymers Division, National Bureau of Standards, Gaithersburg, MD 20899, USA

(Received 22 May 1985)

Neutron scattering measurements were performed on epoxies to elucidate the molecular network structure of these commonly used thermosets. A partially deuterated diglycidyl ether of bisphenol A (DGEBA) was cured with di- and triamines based on poly(propylene oxide) chains. Pronounced neutron scattering peaks were observed on all three epoxies studied, while X-ray scattering yielded scattering typical of most amorphous materials. The neutron scattering results can be explained successfully using equations that have been derived using a result from a random phase approximation based on an ideal network. Neutron measurements were also conducted on epoxies that had been swollen in acetone. The swollen sample results, along with those from the bulk specimens, provide a unique approach to the network homogeneity problem in epoxies.

(Keywords: neutron scattering; epoxy; network; thermosets; topological heterogeneity)

INTRODUCTION

In a previous publication recent results of neutron scattering from partially deuterated epoxies were reported¹. Scattering maxima were observed in all epoxy specimens cured with three different di- or tri- amines. These observed maxima, although they are manifestations of ordering in the epoxy networks, cannot be taken as unequivocal evidence concerning the homogeneity of the network structure within these epoxies tested. In order to answer the question of whether the network structure within epoxies is homogeneous or not, a theoretical development relating the network structure to the corresponding scattered intensities is necessary. The basic approach undertaken here emphasizes the amorphous nature of epoxies, in that it assumes that the correlation of a segment belonging to an average network to its physically contacting neighbours has a typical, liquid-like disorder. Such an assumption enables the use of certain results from a random phase approximation (RPA) to relate an amorphous structure to its scattered intensities²⁻⁴.

The observation of maxima in the neutron scattering results indicates the existence of structural order in these amorphous materials. This structural order must be of an intra-network nature, since the inter-network correlation is assumed to be liquid-like. For example, in the vicinity of any bisphenol A unit there are other bisphenol A units all of which are randomly distributed with respect to the reference unit, except for the ones with an immediate chemical connection. (Because every single molecule within a fully cured epoxy may belong to a giant network, the word 'immediate' refers to connection by a small number of bonds.) The basic assumption is that, if it takes many steps for a chain to return to its starting place, the correlation has been lost.

Therefore one can describe the intensity scattered from epoxies in terms of an intra-network correlation function. A random phase approximation (RPA) is used to derive a basic scattering expression that accounts for the liquid-like disorder of the physical contacting neighbours.

No attempt was made in this work to derive an analytical form for the intra-network correlation function, even for an ideal lattice of infinite molecular weight. Instead, an approximation was used to account for the fact that the correlation within a network persists over a significantly longer distance than the persistence length of an unlinked linear chain.

To justify the use of RPA over the q region of interest, X-ray scattering measurements were also performed on the specimens used in the neutron scattering study. (q is the magnitude of the scattering vector defined as $4\pi/\lambda \sin \theta$. λ is the wavelength and θ is the scattering angle defined in the ordinary manner.)

If the scattering curve of the epoxy in the bulk can be interpreted analytically, one can then address the question of the homogeneity of the network within the epoxy. For epoxies, the terms 'homogeneity' and alternatively 'heterogeneity' require some clarification because there are two types of heterogeneity. The first one is density fluctuation, which includes air bubbles, cracks, impurities of a large scale and frozen-in thermal fluctuations. This type of heterogeneity can be easily measured using X-ray scattering. The other type concerns the uniformity of the molecular network, because an epoxy composed of non uniform networks might nevertheless have very little density fluctuation. Consequently, X-ray measurements on unlabelled specimens provide no information bearing on the question of the network homogeneity.

For an idealized network, each crosslink point possesses an identical number of branches, or the same functionality, and each linkage between two crosslinks has an identical length. Deviations from this idealized case can occur in epoxies, even when the epoxy and the amine are mixed in their stoichiometric ratio. The possible causes include (a) a broad molecular weight distribution in either the epoxy or the amine or both, (b) side reactions other than the intended amine-epoxide reaction, e.g. the homopolymerization of the epoxies and incomplete reaction, (c) topological defects, in the network, e.g. ring formation or loose linkages.

It is the purpose of this work to develop a scheme to measure the heterogeneity in the molecular network of epoxies. Once developed, this scheme will also be applicable to other thermosets and similar crosslinked materials.

The network heterogeneity caused by (a) and (b) can be readily detected from neutron scattering results from specimens in which either the epoxy or the amine has been deuterated because both will give rise to fluctuations in the concentrations of the deuterated and hydrogenated species with the scattering volume. The term 'compositional fluctuation' is chosen hereafter to denote such a case. For an idealized network, the compositional fluctuation is zero, as is the zero angle scattered intensity aside from the density fluctuation contribution. For specimens with a significant amount of compositional fluctuation, one will observe a certain amount of the zero angle scattered intensity. A quantitative relation between the zero angle intensity and the amount of compositional fluctuation is provided later in this work.

The absence of compositional fluctuation does not mean that the network is free of topological defects. Accordingly, the absence of zero angle intensity from a solid specimen is not a sufficient condition for an ideal network structure. However, materials with significant amount of zero angle intensity, hence compositional fluctuation, are likely to contain topological defects. The scheme used in this work to monitor for topological defects within epoxies is to perform neutron scattering measurements on partially deuterated specimens swollen by solvent. Topological defects manifest themselves by inducing some variations in the local swelling ratio. This variation causes scattering intensities in addition to that caused by density and compositional fluctuations.

This paper describes X-ray measurements in bulk specimens and neutron scattering measurements in both bulk and swollen specimens that were performed in order to elucidate the nature of the heterogeneity in epoxies. The experimental procedure is described in the next section. That is followed by a theoretical development of equations describing the scattering for network structures. Finally, both the experimental and theoretical results will be presented, and the problem of the network homogeneity will be addressed.

EXPERIMENTAL

Specimen preparation

DGEBA was chosen as the model epoxy for the present study. To provide neutron scattering contrast, all the hydrogen atoms within bisphenol A were replaced by deuterium. Detailed procedures for synthesizing the deuterium labelled DGEBA have been covered in a previous publication¹. Jeffamine† D-400, D-2000 and T-403 were used as the curing agents. The D-series amines are difunctional primary amines linked by poly(propylene oxide) (PPO); the designation number refers to the approximate molecular weight of each species. T-403 is a tri-functional primary amine, also linked by PPO. The

polydispersities of the polyether glycols, the precursors of these amines, are listed in Table 1. The curing kinetics of this epoxy-amine system have been investigated extensively by others⁵. Their results strongly suggested that the epoxide groups reacted primarily with the amine, and that very little side reaction takes place in this epoxy-amine system. Therefore, the molar ratio of the epoxide to amine was kept at 2:1, the stoichiometric ratio, throughout this work.

The epoxy monomer and the amine were mixed at room temperature and degassed in vacuum for 5 min. The mixtures containing D-400 and T-403 were then placed in a 95°C oven for 24 h. For D-2000 mixture a curing time of 48 h was required at this curing temperature to ensure the completion of cure. In order to obtain a neutron scattering curve for freshly mixed D-2000/epoxy, a sample of this mixture was simply degassed and kept in a quartz cell at 0°C.

In order to determine the amount of heterogeneity within these epoxy specimens, neutron scattering measurements on solvent swollen specimens were also undertaken. Acetone as the solvent was chosen because it has the same relative atomic composition, hence the same scattering cross-section, as that of the PPO. Fully cured epoxy specimens were immersed in acetone until a constant weight was reached. The swollen specimens were then placed inside sealed quartz cells for neutron measurements. A small amount of free acetone was kept inside the cell, but outside the neutron beam, to maintain the epoxy in its equilibrium swelling state. The swelling ratios, defined as the swollen specimen weight divided by the dry weight, were 2.05, 1.51 and 1.20 for the D-2000, D-400 and T-403 epoxies, respectively.

Neutron scattering

All the scattering experiments were carried out at the neutron facilities of the NBS reactor. Two instruments have been used for this work; a 3-axis diffractometer designated as BT-6 and a 3-metre small-angle scattering (SANS) instrument. The analyser crystal of BT-6 was set at its elastic diffraction condition so that the inelastic component of the beam scattered from the specimen was filtered out. In any hydrogen rich material, such as the partially deuterated epoxies, a significant portion of the incoherent scattered intensities is inelastic. Consequently an appreciable amount of the incoherent scattering was excluded from the raw intensities measured with BT-6. Maxima and other minute features on the scattering curves appear very prominently even before any background subtraction. Furthermore, the high-angle region can be covered readily with BT-6 due mainly to the wavelength available, which has a lower limit of about 1 Å, as compared with 5 Å on the SANS instrument. However, a quantitative interpretation of the BT-6 results is rather difficult, since the amount of inelastic

Table 1 Polydispersity of the polyether glycols, the precursors of Jeffamines*

	M_w/M_n
D-400	1.06
D-2000	1.02
T-403	1.13

* Data obtained from H. G. Waddill of Texaco Chemical Co.

† Trade name from Texaco Chemical Co. Certain commercial materials and equipment are identified in this paper to specify adequately the experimental procedure. In no case does such identification imply recommendation or endorsement by the National Bureau of Standards, nor does it imply necessarily that the materials or equipment identified are the best available for the purpose.

scattering increases with scattering angle even though the incoherent contribution to the total scattering is angle independent. To remove the angle independent incoherent background from a hydrogen rich specimen is our main concern, and this can be done more easily from the SANS data. The upper limit of the q value attainable with the 3 metre SANS station is about 0.52 \AA^{-1} when the shortest specimen to detector distance of 2 metres was used. For higher q values up to 1.2 \AA^{-1} , one has to refer to the results from BT-6 data which were collected from all three epoxy-amine systems.

The raw data from SANS contains both the coherent and incoherent components. We first performed a SANS measurement from a solvent mixture of the same chemical composition as the test specimen. The ratio of the incoherent to the total scattered intensities was calculated by summing up the incoherent cross-sections of all the constituent atoms within the solvent mixture. The incoherent component was then estimated from the intensities scattered from the solvent mixture at high q values.

X-ray scattering data over a q region of 0.1 to 1.5 \AA^{-1} were also obtained on all three epoxy/amine specimens. The copper $K\alpha$ line from a conventional X-ray source was used, and the detection system used was a linear position sensitive detector (l.p.s.d.) manufactured by TENNELEC. Air scattering was subtracted from all the epoxy scattering curves to be reported.

Theoretical development in scattering from epoxies

An expression based on an ideal network model for the intensities scattered from epoxies will be derived in this section. The basic assumption inherent in such a model is that, for any specific structural unit, (the deuterated bisphenol A was arbitrarily chosen) the surrounding units of the same kind are randomly distributed except for the ones connected chemically to it. This assumption is depicted in *Figure 1a* for epoxy networks composed of the D-series amines. The corresponding chemical structure of the linkages is given in *Figure 1b*, where the deuterated bisphenol A is denoted by the solid dot. It was chemically linked to others by amines in the cured epoxies. Only one part of an ideal network is shown in the above Figure. Surrounding an arbitrarily chosen unit 1 there are numbers of other randomly distributed structure units which belong to other networks similar to the one shown. In the limiting case that nearly all the neighbouring units are uncorrelated, such as in the case of linear polymers, the scattering intensities can be expressed in the same form as that developed for linear block copolymers².

$$I(q) = (\alpha_1 - \alpha_2)^2 \frac{X_1(q)X_2(q) - X_{12}^2(q)}{X_1(q) + X_2(q) + 2X_{12}(q)} \quad (1)$$

where $X_1(q)$ is the Fourier transform of the correlation function of all the deuterated units within an average network, and $X_2(q)$ is the counterpart of $X_1(q)$ for the hydrogenated species, which consists primarily of PPO units. These two structural units are differentiated by their scattering cross-sections α_1 and α_2 . $X_{12}(q)$ is the cross term among all the units 1 and 2 of the same network. The detailed definition of $X_1(q)$, $X_2(q)$ and $X_{12}(q)$ can be found elsewhere⁴. It is evident that the scattering expression for the unit shown in *Figure 1a* will deviate from equation (1)

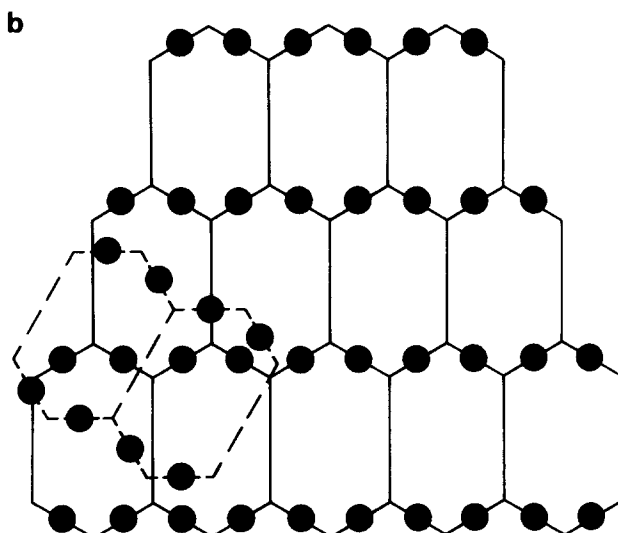
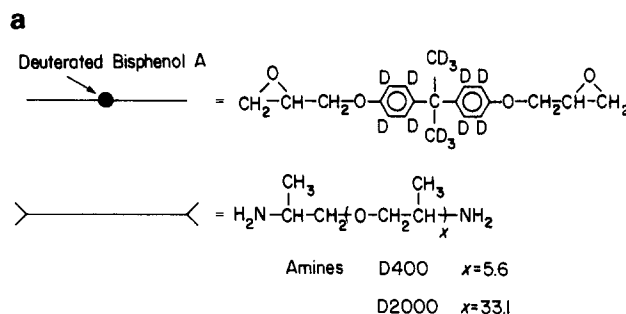


Figure 1 (a) The chemical compositions of the deuterated DGEBA and the D-series amines. These molecules are represented by thin lines and dots shown in the left hand side. (b) An idealized network model of the epoxies made from the deuterated DGEBA and the D-series amines

as the mesh size decreases. The resultant limiting case is described by the expression

$$I(q) = \alpha_1^2 X_1(q) + \alpha_2^2 X_2(q) + 2\alpha_1\alpha_2 X_{12}(q) \quad (2)$$

Inorganic glasses and many crystalline materials are good examples of what is represented by equation (2). In the epoxies studied in this work, equation (1) applies, since the chain length of the amine, or the mesh size, is significantly greater than the cross-sections of the constituent molecules. As the mesh size decreases to the extent that a significant fraction of the physical neighbours of an average unit consist of its topological neighbours, the scattering behaviour will lie somewhere between that represented by equations (1) and (2). No formal derivation of the scattering expression for such an intermediate state is available. If one expects a smooth transition between equations (1) and (2), it is reasonable to assume that the intensity can be expressed in the form

$$I(q) = f(\psi)I_1(q) + (1-f(\psi))I_2(q) \quad (3)$$

where the subscripts 1 and 2 refer to intensities derived from equations (1) and (2), respectively, ψ denotes the volume fraction occupied by the chemical repeat units within an average mesh, and $f(\psi)$ is an undefined function of ψ .

Now expressions for $X_1(q)$, $X_2(q)$ and $X_{12}(q)$ will be derived, based on an ideal network model as shown in *Figure 1*. To facilitate the derivation one divides an

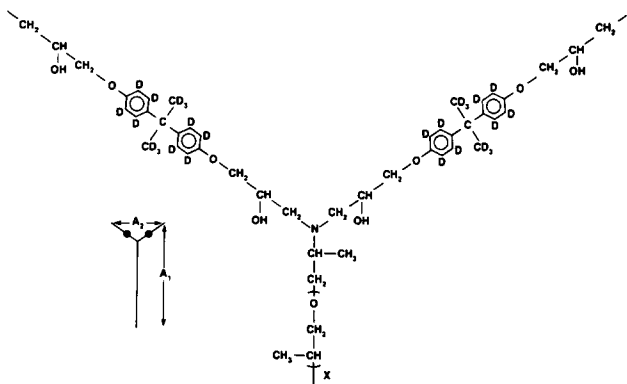


Figure 2 A unit cell and its corresponding chemical composition to make up the network shown in Figure 1b

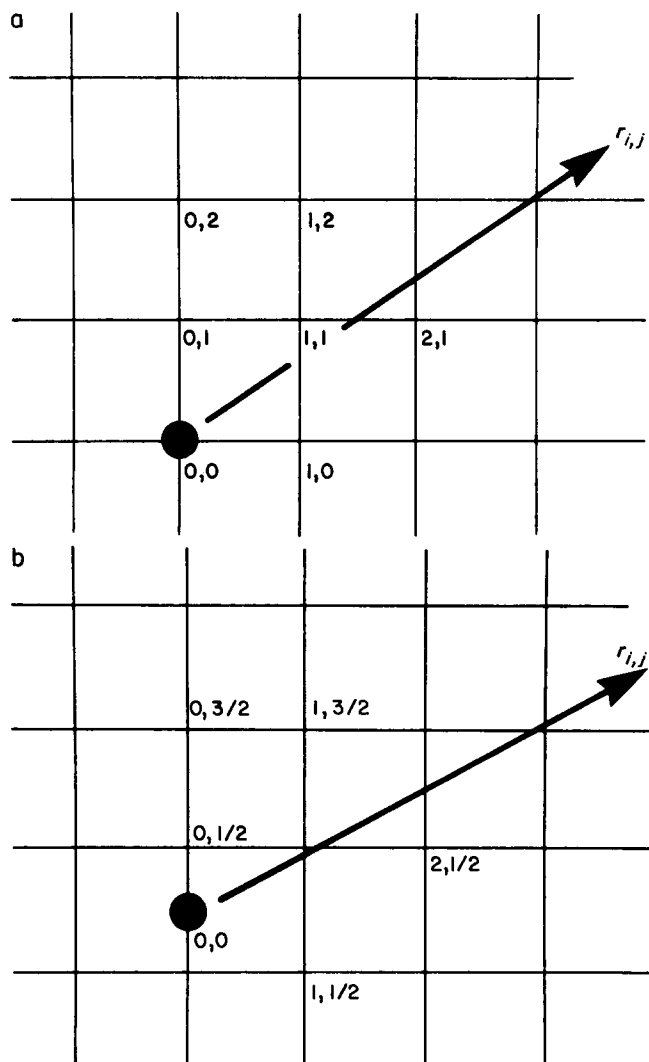


Figure 3 (a) Lattice structure used as an intermediate step in the calculation of the self correlation functions $X_1(q)$ and $X_2(q)$. (b) The lattice structure used in the calculation of the cross correlation function $X_{1,2}(q)$

average network into unit cells. In the cases for D-2000 and D-400 epoxies, the ideal structure for an exclusively amine/epoxide reaction product can be depicted as in Figure 1. The unit cell was chosen as in Figure 2a and the corresponding lattice is given in Figure 3a.

Hereafter, $X_1(q)$ and $X_2(q)$ can be written as

$$X_1(q) \approx \langle f_1^2(q) \rangle + \langle f_1(q) \rangle^2 \left\langle \sum_{i,j=1}^{\infty} \frac{\sin qr_{ij}}{qr_{ij}} \right\rangle \quad (4)$$

and

$$X_2(q) \approx \langle f_2^2(q) \rangle + \langle f_2(q) \rangle^2 \left\langle \sum_{i,j=1}^{\infty} \frac{\sin qr_{ij}}{qr_{ij}} \right\rangle \quad (5)$$

where expressions $f_1(q)$ and $f_2(q)$ are the form factors of structure units 1 and 2, respectively, and $\langle \rangle$ denotes an average over all orientations and molecular weights. Unit 1 is represented by the two heavy dots of Figure 2 and unit 2 is composed of the remaining chemical constituents in the same Figure. The term with double summation denotes the form factor of the infinite lattice shown in Figure 3a.

Certain approximations inherent in equations (4) and (5) require further discussion. These equations imply that no orientational correlation exists, even between any two adjacent structural units. For an ideal rigid lattice, where the orientational correlation persists over a large lattice space, the term with $\langle f_i(q) \rangle^2$ should be replaced by $\langle f_i(q)^2 \rangle$. In the present case of a flexible lattice, we adopt expressions (4) and (5) as an approximation.

By using the same scheme as outlined above, an expression for $X_{1,2}(q)$, the intercorrelation between units 1 and 2 within the same network, can be written as follows:

$$X_{1,2}(q) \approx \langle f_1(q) \rangle \langle f_2(q) \rangle \left\langle \sum_{i,j=1}^{\infty} \frac{\sin qr_{ij}}{qr_{ij}} \right\rangle \quad (6)$$

where the double summation is carried out on the lattice given in Figure 3b which is different from that of Figure 3a. Throughout the summation the origin of r_{ij} is fixed at position (0,0) of Figure 3b. The same approximation of a total absence of orientational correlation among the adjacent structural units is also implied in equation (6).

The value of r_{ij} appearing in equations (4), (5) and (6) denotes the distance between the lattice origin and the (i,j) node on the network or the lattice. Even if the nodes are interconnected by flexible chains, PPO in this case, the nodes within a network are expected to be highly correlated or localized, as has been shown by others^{6,7}. In other words, the value of $\langle r_{ij}^2 \rangle$ is greater than that of a linear Gaussian chain, even if the linkage might follow a Gaussian behaviour when unlinked. At the other extreme, a rigid network, the value of $\langle r_{ij}^2 \rangle^{1/2}$ is simply $(i^2 A_1^2 + j^2 A_2^2)^{1/2}$ where A_1 and A_2 are the average distances between two adjacent nodes along the $(PPO)_n$ chain and the epoxide-amine-epoxide bonds, respectively (Figure 2a).

In the present case, the value of r_{ij} is believed to be somewhat less than $(i^2 A_1^2 + j^2 A_2^2)^{1/2}$, which is denoted L_{ij} . The deviation in position of the node from an ideal and infinitely rigid network is expected to increase gradually as the value of $|i| + |j|$ increases. One could adopt the paracrystalline model proposed by Hoseman⁸ to approximate the value of r_{ij} , but the resultant scattering curve does not match the experimentally observed one. More explicitly, the shoulder at $q = 0.24 \text{ \AA}^{-1}$ can not be reproduced by such a model in D-2000 epoxy. Consequently, an alternative approach is chosen in which one relates the quantities r_{ij} and L_{ij} through a Porod-Kratky⁹ function developed for semi-rigid long chain molecules. There is a major difference between the paracrystalline and Porod-Kratky models, in that independent steps are assumed to connect all adjacent nodes in the former model, whereas the latter one can only allow for a gradual variation among steps connecting nodes. The persistence length, P ,

in a Porod-Kratky model for the present case is therefore expected to be greater than either A_1 or A_2 , the average step lengths along the amine and epoxide chains, respectively. The value of P in the epoxy is also much greater than it is in the constituent polymer in its isolated linear form, due to the constraint or localization of the crosslinks. Under the premise of a large P , the mean and the square mean of the quantity r_{ij} can be approximated in accordance with the main Porod-Kratky results as follows:

$$\langle r_{ij} \rangle \approx P \left[1 - \exp\left(-\frac{L_{ij}}{P}\right) \right] \quad (7)$$

and

$$\langle r_{ij}^2 \rangle \approx 2P \left[L_{ij} - P \left(1 - \exp\left(-\frac{L_{ij}}{P}\right) \right) \right] \quad (8)$$

The fluctuation of r_{ij} around its mean value, $\langle r_{ij} \rangle$, can be calculated from the relation $\langle \delta_{ij}^2 \rangle = \langle r_{ij}^2 \rangle - \langle r_{ij} \rangle^2$. The double summation in equations (4), (5) and (6) can be simplified with a Gaussian approximation as

$$\left\langle \sum_i \sum_{j=1}^{\infty} \frac{\sin qr_{ij}}{qr_{ij}} \right\rangle \approx \sum_i \sum_{j=1}^{\infty} \frac{\sin q \langle r_{ij} \rangle}{q \langle r_{ij} \rangle} \exp\left(-\frac{q^2 \langle \delta_{ij}^2 \rangle}{2}\right) \quad (9)$$

Thus, the scattering curves of networks in the bulk state can be calculated with input parameters A_1 , A_2 and P which are the unit step length along the amine, and epoxide and the persistence length of the network.

The terms $\langle f_i^2(q) \rangle$ and $\langle f_i(q) \rangle$ in equations (4) to (6) are approximated as

$$\langle f_i^2(q) \rangle \approx \langle N_i \rangle^2 P_{\langle N_i \rangle}(q) \quad (10)$$

$$\langle f_i(q) \rangle \approx \langle N_i \rangle \frac{12}{U_i} \left[1 - \exp\left(-\frac{U_i}{12}\right) \right] \quad (11)$$

where $i=1$ or 2 , N_i is the molecular weight of type i between the crosslinks $P_{\langle N_i \rangle}(q)$ is the Debye function based on the average molecular weight $\langle N_i \rangle$, and U_i stands for $\langle N_i \rangle q^2 l_i^2$ where l_i is the segment length and is chosen to be 2.7 \AA , which is, approximately the length of a PPO unit¹⁰. The molecular weight is scaled in such a way that the molecular weight of acetone is unity. The expression for $\langle f_i(q) \rangle$ is simply a Fourier transform of a Gaussian chain about its central segment.

Equations (10) and (11) represent a rough approximation for the conformation of a linear chain connecting two crosslink points. Even when the functionality is only three, as in the present case, one still expects the segment density distribution of a linkage to be somewhat depleted near the crosslinks. Such a case has been treated by Daoud and Cotton for star polymers¹¹. On this basis, equations (10) and (11) are adopted in lieu of the expression for a linear Gaussian chain with an end to end distance A_i .

For specimens cured with Jeffamine T-403 the network structures are too complicated to be depicted by any diagram similar to that in *Figure 1*. Although the general equations (1)–(3) are still expected to be applicable to the T-403 containing epoxy, the analytic expressions for $X_1(q)$, $X_2(q)$ and $X_{12}(q)$ are difficult. Part of the difficulty arises because unlike the linear amines, no single obvious ideal network can be identified. Under the assumption of

an exclusive epoxide-amine reaction as in the previous example, the 'unit cell' of the T-403 epoxide is given in *Figure 4*. The configuration, hence the scattering function, will depend on the characteristic lengths A_1 , A_2 and the persistence length P , as defined earlier. The magnitude of A_2 is the same as in *Figure 2* for D-400 and D-2000 epoxies, while A_1 in the present case is expected to be somewhat less than that of D-400 epoxy. This is due to the fact that the combined molecular weight of any two of the branches in T-403 is less than that of D-400. Although no explicit expression will be given for the scattering function of T-403 epoxy, the general characteristics of the scattering curves between T-403 and D-400 are expected to be similar.

The scattering measurements on epoxies by solvent were performed to elucidate the topological homogeneity of the network. In a swollen ideal network, the concentration fluctuation of the solvent molecules is expected to have a characteristic length similar to the mesh size. A mean field approximation is therefore viable in this situation. The atomic composition of acetone, used as the solvent, is identical to PPO, the basic structural unit of all the amines used herein. This results in equality of the scattering cross section between the amines and the solvent which is denoted as component 3. The corresponding scattering equations from a mean field approximation for a swollen network (Appendix) is

$$I(q) = (\alpha_1 - \alpha_2)^2 \frac{X_3(q)X_2(q) + X_1(q)X_2(q) - X_{12}^2(q)}{X_1(q) + X_2(q) + X_3(q) + 2X_{12}(q)} \quad (12)$$

Owing to the size of the solvent molecules, the term $X_3(q)$ can be approximated as ϕ_3 , the volume fraction of solvent within the swollen network.

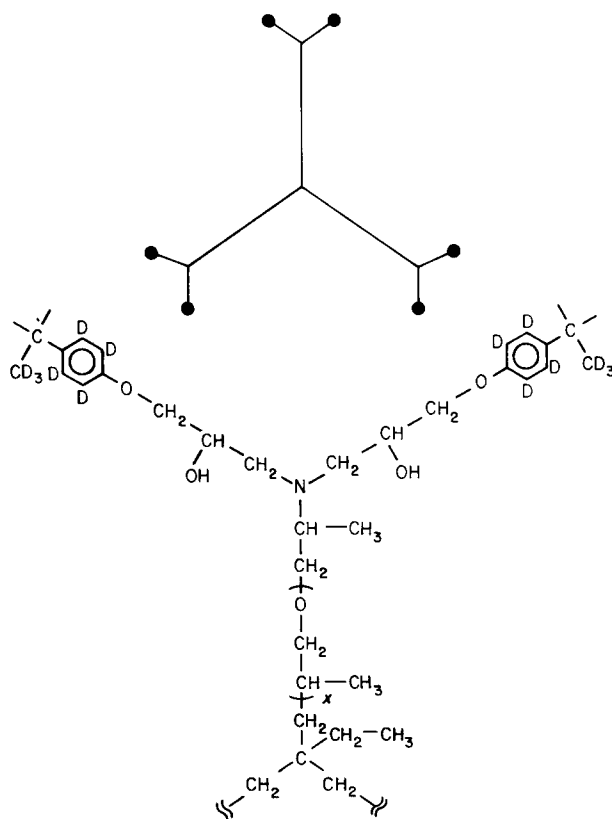


Figure 4 Unit cell for the epoxy made from the deuterated DGEBA and T-403 amine

RESULTS

The X-ray scattering curve of one of the D-2000 containing epoxy specimens used in neutron measurements is shown in *Figures 5a* and *b*. A broad scattering maximum in the q region of 1.2 \AA^{-1} is the only prominent feature. Such a broad maximum is rather typical of amorphous solids, e.g. fused silica. The scattering curves from the other two amine containing epoxies are identical to those shown in *Figure 5*. The neutron scattering results obtained from SANS on the D-2000 epoxy in the bulk and the swollen states are shown in *Figure 6a* and the results from the 3-axis diffractometer (BT-6) are given in *Figures 6b* and *c*. *Figure 6b* demonstrates the evolution of the scattering curves as cure proceeds; the cumulative cure time is marked on each curve. *Figure 6c* presents the scattering intensities of fully cured specimens after subtracting the empty cell intensities. A qualitative similarity between the SANS and the BT-6 results is apparent: a pronounced peak at $q=0.13 \text{ \AA}^{-1}$, a broad peak around $q=0.40 \text{ \AA}^{-1}$ and a weak shoulder at $q=0.24 \text{ \AA}^{-1}$. The existence of a shoulder at 0.24 \AA^{-1} can be seen in both the BT-6 results and SANS result covering the same q region as shown in *Figure 6a*. *Figure 6d* gives the difference in scattering intensities between the 12 h cured specimen and the fresh one. The negative intensity near the low q region indicates a significant decrease in compositional fluctuation as the cure proceeds. The excess intensity beyond $q=0.15 \text{ \AA}^{-1}$ indicates certain structure formation resulting from cure. Owing to the difficulty of removing

the incoherent contribution, as mentioned in a previous section, the BT-6 data will only be viewed as a reference, and only the data from SANS will be considered in quantitative discussions. All the SANS data reported in this work have been normalized to the same monitor count, specimen thickness, and absorption corrections. A flat background attributed to incoherent scattering has also been removed according to the procedure mentioned in the experimental section.

The experimental results for D-400 and T-403 epoxies in both the bulk and the swollen states are shown in *Figures 7* and *8* respectively. A single maximum is the common feature for these two epoxies in their bulk states. The slight increase of the scattered intensities near $q=1.2 \text{ \AA}^{-1}$ for the bulk specimens, shown in *Figures 7b* and *8b*, is due to the density fluctuation as determined by the X-ray results of *Figure 5*.

A theoretical curve matching these peak positions for D-2000 epoxy in the bulk state is shown in *Figure 9a*. The parameters used to fit the experimental results are $A_1=43 \text{ \AA}$, $A_2=16.5 \text{ \AA}$ and $P=300 \text{ \AA}$, together with an M_w/M_n value of 1.02 (from *Table 1*). To illustrate the effect of these parameters on the shape of the scattering curve, a set of curves with systematic changes in all variables is given in *Figures 9b* and *c*. Basically, the positions of the primary peak at 0.13 \AA^{-1} and the shoulder at 0.24 \AA^{-1} are determined by the value of A_1 , and the value of P affects the sharpness of the 0.13 \AA^{-1} peak. A high value of P , corresponding to a rigid network, results in well defined peaks. The value of 300 \AA for P was chosen to match the width of the main peak at 0.13 \AA^{-1} . The value of A_2 dominates the peak position at 0.4 \AA^{-1} . The theoretical result for D-400 in the bulk state is presented in *Figure 9d*, in which a polydispersity value of 1.13 (from *Table 1*) was used, and 21 \AA was chosen for both A_1 and A_2 in order to match the peak position. The value of P , the persistence length, was chosen to be 300 \AA as in the case of D-2000. The most striking difference between the experimental and calculated results for the bulk specimens (*Figure 6a* vs. *Figure 9a*, *7a* vs. *9d*) is the zero angle intensity; the calculated curve goes to zero whereas the experimental curve goes to a finite value. This discrepancy is significant and will be dealt with in a later section.

The changes in the scattering intensities for these three epoxies upon swelling by acetone are also shown in *Figures 6a*, *7a* and *8a*. The corresponding theoretical predictions from equation (12) are also given in *Figures 9a* and *9d*. The swelling ratio was measured to be 2.05, 1.51 and 1.20 for epoxies D-2000, D-400 and T-403, respectively. By assuming the mesh size of the network, or more explicitly, that the values of A_1 and A_2 increase affinely with the bulk swelling ratio, one obtains the theoretical curves given in *Figures 9a* and *10*. The value of the persistence length P is assumed to hold constant upon swelling. It is conceivable that swelling will result in an increase in P . However, a small change in P will not affect the shape of the scattering curves. The prominent features in the experimental scattering results of these swollen epoxies are: (1) a shift of the first maximum to a lower q region for D-2000 and T-403 cases, the amount of shift being close to what an affine deformation will predict, as judged from the theoretical results, and (2) an increase of the zero angle scattering intensities upon swelling. For the D-400 cured epoxy, the amount of the peak shift upon swelling is difficult to estimate from the experimental

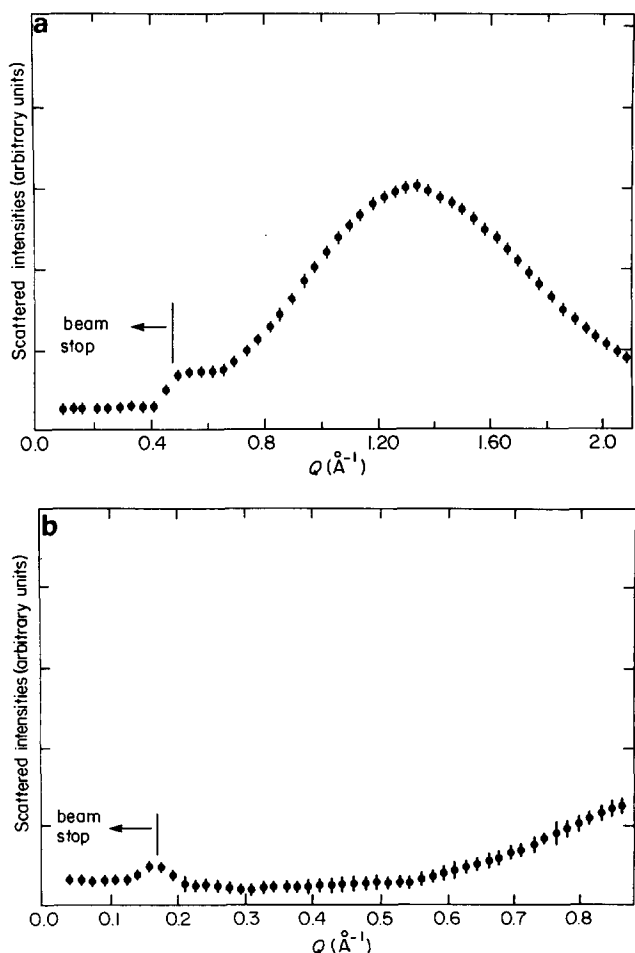


Figure 5 (a) X-ray scattering result of D-2000 epoxy specimen. Air scattering contribution has been subtracted. (b) Same as *Figure 5a* but in a lower q region

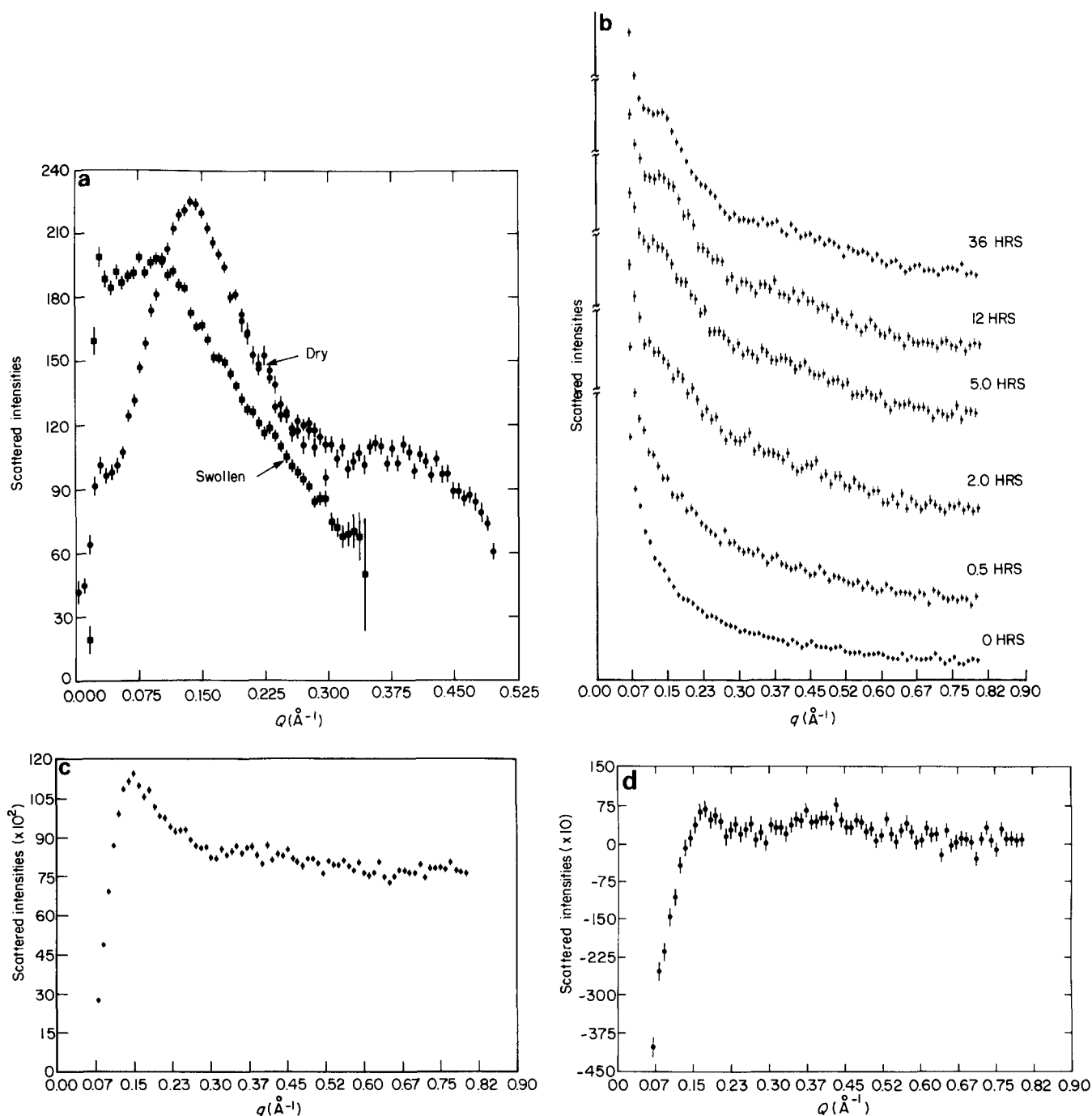


Figure 6 (a) Neutron scattering curves of both the dry and the acetone swollen D-2000 epoxy. The swelling ratio is 2.05. Data obtained from the SANS station and the incoherent contribution has been subtracted. (b) Neutron scattering curves (raw data) of the D-2000 epoxy as a function of the cure time. The cumulative cure time was marked on each respective curve. Data obtained from BT-6 diffractometer. (c) Neutron scattering curve of a fully cured D-2000 epoxy after the empty cell subtraction. Data obtained from BT-6. (d) Difference in the scattered intensities between the 12 h cured specimen and the zero hour one shown in Figure 6a. The development of the correlation hole is evident from the negative intensities near zero q

result. Once again the theoretical prediction calls for the intensities near $q=0$ to decrease slightly instead of increasing upon swelling as shown in Figure 9a. This discrepancy plays a critical role determining the extent of the network homogeneity in epoxies, and it will be addressed in a later section.

In most of the theoretical results, anomalies are present near both the zero angle and the onset of the first maximum. The relatively low theoretical intensities in the low q region arise from the subtraction of the terms, $X_1(q)X_2(q)$ and $(X_{12}(q))^2$. The values of both these terms in the low q region are at least one order of magnitude higher than that of the maximum resulting from their subtraction and shown in the final curves. In all the

theoretical results given in this work, the computation was limited to a lattice with 400 repeating units. Consequently, one can not expect a perfect cancellation between $X_1(q)X_2(q)$ and $(X_{12}(q))^2$ in the low q region.

DISCUSSION

The X-ray result of Figures 5a and b demonstrates that the epoxies tested herein are amorphous; for any atom chosen at random its neighbouring atoms are irregularly packed. More specifically, the lack of zero angle intensity of the X-ray results indicates that the incompressibility assumption leading to the scattering expression of equation (1) is valid. The q range over which the incompressibility assumption

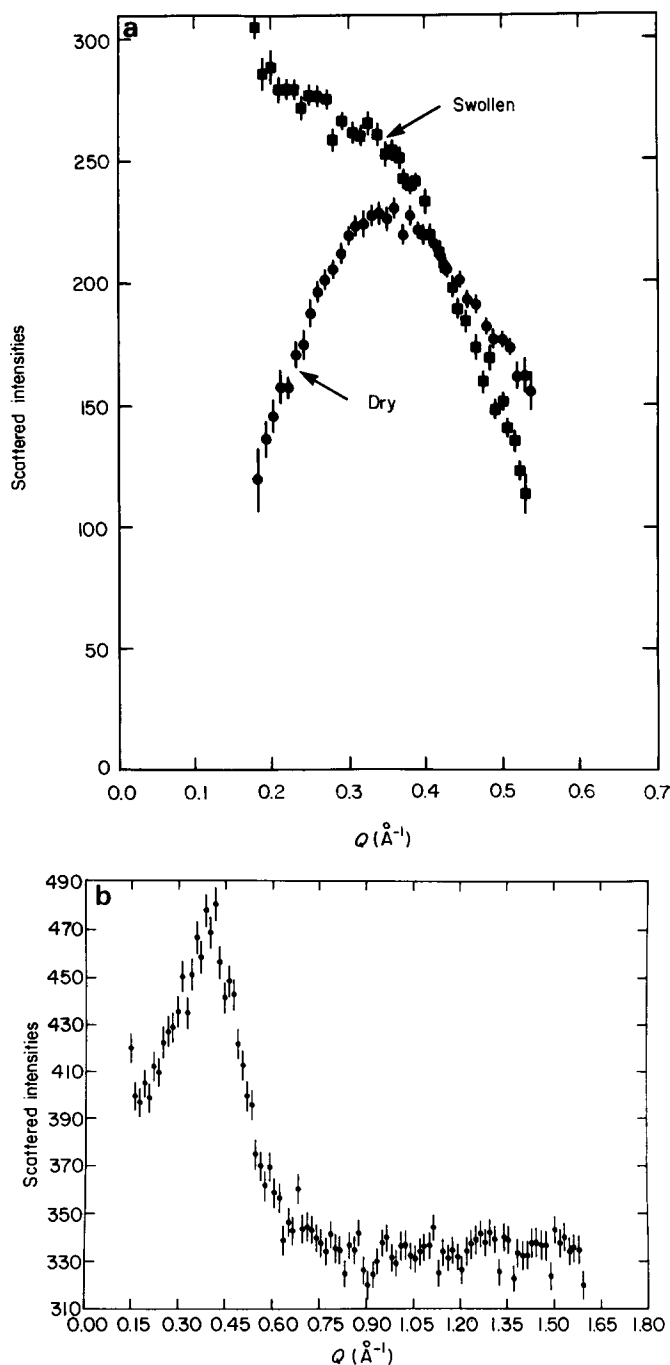


Figure 7 (a) Neutron scattering curves of a D-400 epoxy in both the dry and the acetone swollen states. The swelling ratio is 1.51. Data after subtracting the incoherent contribution. Data obtained from SANS station. (b) Neutron scattering curve (raw data) of a D-400 epoxy. Data obtained from BT-6 diffractometer to cover a broad q region

fails severely is around 1.2 \AA^{-1} , which is rather remote from the q range of major interest in this work.

In order to justify the use of equation (1) instead of (2) for data interpretation the value of ψ , the volume fraction occupied by a repeat unit within a unit cell, is needed. It is desirable for the ψ value to be substantially below 1.0. The ψ value can be estimated from the unit cell dimensions A_1 and A_2 , along with the molecular weight of a repeat unit. The values of A_1 and A_2 used to simulate the experimental results are tabulated in Table 2. By letting the volume of a unit cell be $(A_1 A_2)^{3/2}$ and the density of the epoxy be 1.2 g/cm^3 , the estimated values of ψ are 0.172

and 0.113 for D-2000 and D-400, respectively. The magnitude of ψ for both cases tends to justify the use of equation (1) for treating the epoxies studied herein.

The discrepancy between the theoretical result and the observed scattering intensities at zero angle can be explained as follows. The observed neutron scattered intensities at zero angle are proportional to the concentration fluctuation of either the deuterated or the hydrogenated species within the scattering volume. This fluctuation arises from two different sources, the density fluctuation in the specimen and the compositional fluctuation. The former can be neglected over the q region below 0.5 \AA^{-1} , as justified by the X-ray results of Figure 5a. As to the compositional fluctuation, for the ideal

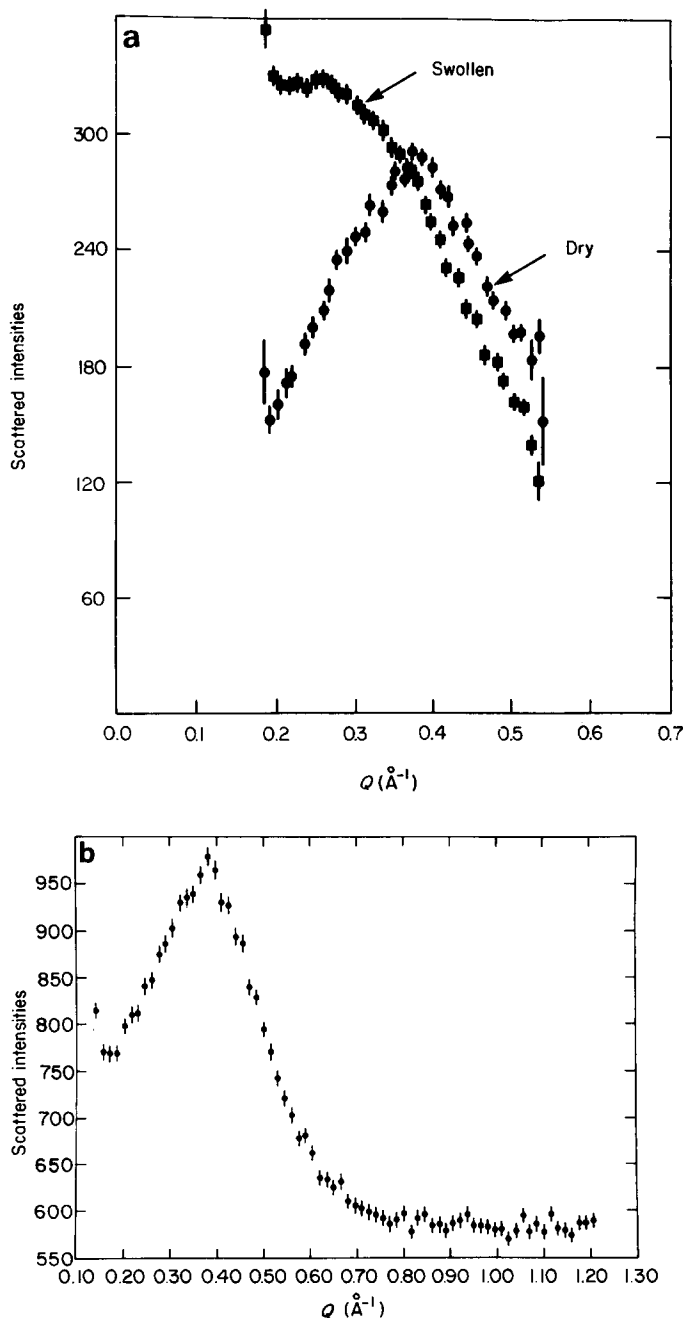


Figure 8 (a) Neutron scattering curves of a T-403 epoxy in both the dry and the acetone swollen states. The swelling ratio is 1.20. Data after subtracting the incoherent contribution. Data obtained from SANS station. (b) Neutron scattering curve (raw data) of a T-403 epoxy. Data obtained from BT-6 diffractometer to cover a broad q region

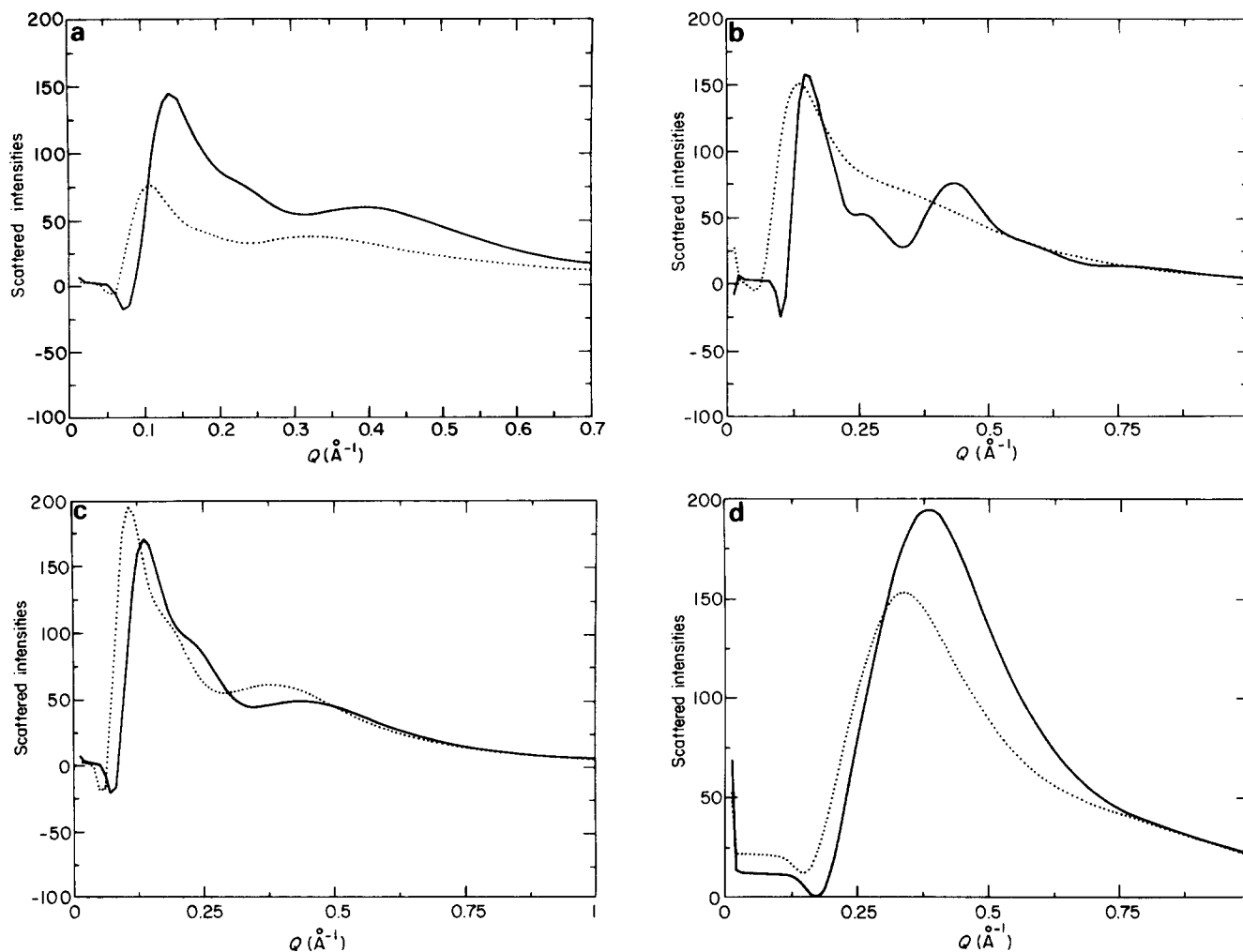


Figure 9 (a) Theoretical scattering curves of D-2000 epoxy in both the dry (solid line) and the acetone swollen (dotted line) states. For the dry specimen, $A_1 = 43 \text{ \AA}$, $A_2 = 16.5 \text{ \AA}$, $P = 300 \text{ \AA}$. For the swollen specimen, $A_1 = 54.6 \text{ \AA}$, $A_2 = 21 \text{ \AA}$, $P = 300 \text{ \AA}$, $\phi_3 = 0.51$. Polydispersity $M_w/M_n = 1.02$ for both curves. (b) Theoretical scattering curves of D-2000 epoxy to demonstrate the effect of persistence length P on the peak shape. $P = 3000 \text{ \AA}$ for the solid curve and $P = 50 \text{ \AA}$ for the dotted curve. $A_1 = 43 \text{ \AA}$ and $A_2 = 16.5 \text{ \AA}$ for both cases. (c) Theoretical scattering curves of D-2000 epoxy to demonstrate the effect of mesh sizes, A_1 and A_2 , on the peak position. $A_1 = 55 \text{ \AA}$ and $A_2 = 16.5 \text{ \AA}$ for the dotted curve; $A_1 = 43 \text{ \AA}$ and $A_2 = 14 \text{ \AA}$ for the solid curve; $P = 300 \text{ \AA}$ for both. (d) Theoretical scattering curves of D-400 epoxy in both the dry (solid curve) and the acetone swollen (dotted curve) states. For the dry specimen, $A_1 = A_2 = 21 \text{ \AA}$, $P = 300 \text{ \AA}$. For the swollen specimen, $A_1 = A_2 = 24 \text{ \AA}$, $P = 300 \text{ \AA}$, $\phi_3 = 0.33$. Polydispersity $M_w/M_n = 1.06$ for both curves

network model depicted in *Figure 1* the only possible cause is variation in the molecular weights of the epoxy and the amines. The g.p.c. results of these three poly(ether glycols), the precursors of the amines used, are given in *Table 1*. The molecular weight distributions are unusually narrow. The enhancement of the zero angle intensity due to a broad molecular weight distribution has been demonstrated in the case of block copolymers^{2,3}, where the density fluctuation is also neglected.

In order to accommodate the observed zero angle intensities, the result of D-2000 epoxy was chosen for fitting with the theoretical work, since some complex scattering features are present in this epoxy. Following the lead from block copolymers, the quantity M_w/M_n was chosen to be 1.5 for both the D-2000 amine and the epoxy. M_w and M_n are the weight and number average molecular weight respectively. These quantities are related to $\langle N^2 \rangle$ and $\langle N \rangle$ of equations (10) and (11) through the simple relations $M_n = \langle N \rangle$, $M_w = \langle N^2 \rangle / \langle N \rangle$. The fit between the theoretical and the observed results is satisfactory, as demonstrated in *Figure 10* for D-2000 epoxy in its bulk state.

An important difference has been implied in the theoretical treatment of the partially deuterated network

compared with linear block copolymers in terms of the molecular weight broadening effects. For block copolymers the local dimensions of a block, for example the end-to-end distance and the radius of gyration, are merely a function of the molecular weight of that specific block, regardless of the molecular weight of the adjacent molecules. This statement is also true for linear polymers at least in a mean field approximation. This simplification can no longer be true for networks because the distance between any two adjacent crosslinks depends not only on the molecular weight of the shortest linkage connecting them, but also on the molecular weight of all the surrounding linkages belonging to the network under consideration. In other words, the distance between two adjacent crosslinks is a function of the molecular weight of many connected linkages in the general vicinity. Consequently, the quantities $\langle r_{ij} \rangle$ and $\langle \delta_{ij}^2 \rangle$ of equation (9) are still calculated using the mean values A_1 and A_2 even though a distribution in molecular weight of the constituent segments is now introduced. More explicitly, one expects that the regularity within networks will not deteriorate as readily as in block copolymers. Consequently, a pronounced peak still persists in *Figure 11*, even after a molecular weight broadening of $M_w/M_n = 1.5$

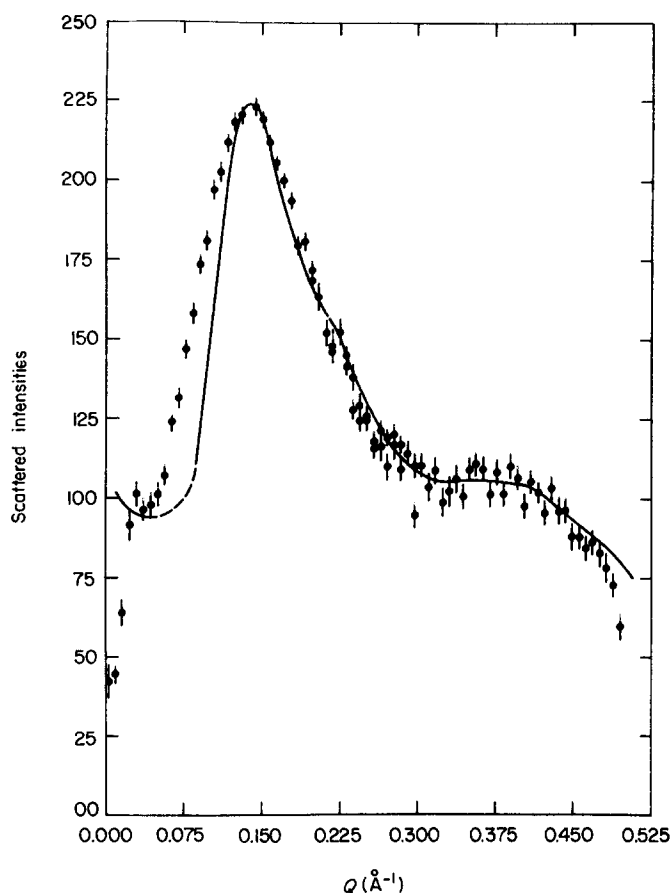


Figure 10 Experimental result (dots) of the dry D-2000 epoxy measured in SANS station together with the theoretical curve (solid line). $A_1 = 43 \text{ \AA}$, $A_2 = 16.5 \text{ \AA}$, $P = 300 \text{ \AA}$, and polydispersity (M_w/M_n) was chosen to be 1.5 to match the observed zero angle intensities

Table 2 Mesh size and the volume fraction (ψ) occupied by a repeating unit within a unit cell

	$A_1(\text{\AA})$	$A_2(\text{\AA})$	$\psi(\%)$
D-400	21	21	11.3
D-2000	43	16.5	17.2

is introduced. For block copolymers the peak degenerates significantly after the same amount of molecular weight broadening is allowed³.

The result of *Figure 10* tends to suggest that the D-2000 epoxy is composed of regular networks in which the segment molecular weight has a broad distribution. However, one other obvious conjecture regarding the epoxy structure also merits consideration, namely, that only a portion of the molecules are incorporated in regular networks while the rest of the molecules are in disarray. Accordingly, the observed scattering curve, for example *Figure 6a* for D-2000, can be decomposed into two components, as demonstrated in *Figure 11*. In addition to the scattering contribution from a regular network there is a background originating from the disordered phase. In this two-phase model no extra molecular weight broadening is needed to accommodate the observed zero angle intensities. Instead, one has to allow for certain curing reactions other than the amine-epoxide reaction. Such side reactions in epoxies are well documented in the literature¹², and they will cause

compositional fluctuation, resulting in the observed zero angle intensities. In the case where only an exclusive amine-epoxide reaction is allowed, the compositional fluctuation must be zero provided the density fluctuation is negligible and the monomers have monodisperse molecular weight distribution. The above remark holds true regardless of the supermolecular structure of these reacted molecules, i.e., whether there is certain network structure or not has no consequence on the above remark.

The experimental results of the acetone swollen epoxies provide additional evidence supporting the two-phase model proposed above. Once again, the D-2000 case will be the focal point of discussion. The swelling ratio of this epoxy is 2.05, and accordingly the average mesh size of the network is increased to 54.6 \AA and 21.0 \AA for A_1 and A_2 respectively. Using equation (12) and a polydispersity value of 1.50 as before, the theoretical result is given in *Figure 12*. The theoretical prediction based on a one-phase, ideal network model calls for a decrease in the zero angle scattered intensities upon swelling. Such a decrease can be easily understood since the solvent is monodisperse and the swelling of an ideal network should be more uniform over a scale larger than the average mesh size. However, the experimental result (*Figure 6a*) points to the contrary; the zero angle intensities increase beyond that of the bulk specimen. On the other hand, the peak position of the swollen specimen is consistent with that predicted from a simple affine calculation. These observed features in the scattering curve can be easily interpreted by the two-phase model as follows. The shift of the peak position

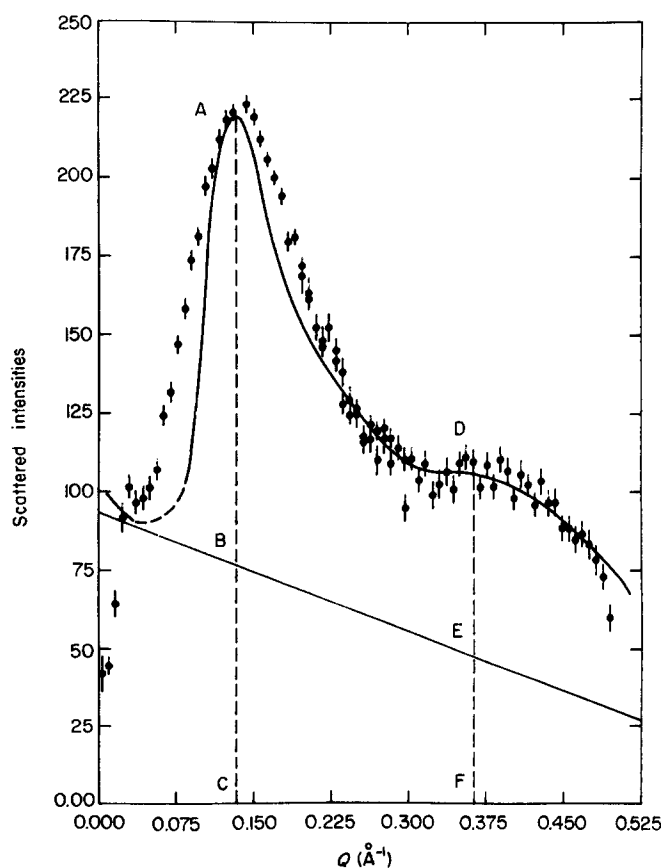


Figure 11 Experimental result (dots) of the dry D-2000 epoxy measured in SANS station together with the theoretical curve (solid line). The experimental result was divided into two portions and the upper one was matched with the theoretical curve, $A_1 = 43 \text{ \AA}$, $A_2 = 16.5 \text{ \AA}$, $P = 300 \text{ \AA}$ and $M_w = M_n = 1.02$

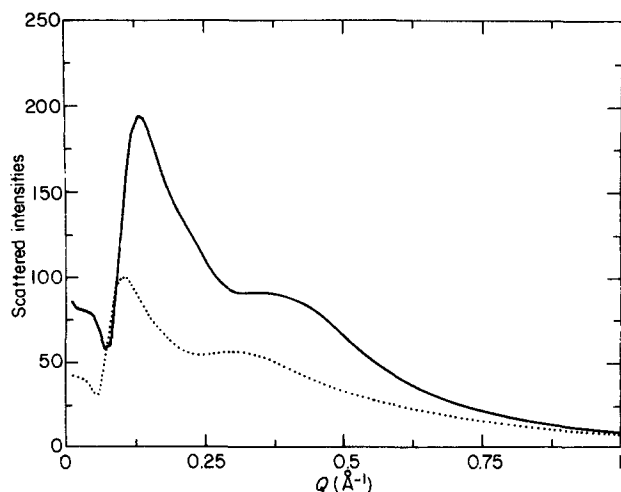


Figure 12 Theoretical scattering curves of D-2000 epoxy in both the dry (solid line) and the acetone swollen (dotted line) states. For the dry specimen, $A_1 = 43 \text{ \AA}$, $A_2 = 16.5 \text{ \AA}$, $P = 300 \text{ \AA}$. For the swollen specimen, $A_1 = 54.6 \text{ \AA}$, $A_2 = 21 \text{ \AA}$, $P = 300 \text{ \AA}$, $\Phi_3 = 0.51$. Polydispersity $M_w/M_n = 1.5$ for both curves

to a small q can be regarded as the evidence that the network portion of the specimen is swollen affinely. The disorder portion must also be swollen, and the corresponding scattering curve from the swollen disordered portion is similar to that of a concentrated polymer solution.

In summary, the results on the bulk D-2000 epoxy specimens indicate the existence of compositional fluctuation. The scattering result from the acetone swollen specimens suggests extensive topological defects in the epoxy network. An exaggerated polydispersity of the monomers is adequate to accommodate the bulk specimen result but fails to account for the swollen specimen result.

The theoretical results for the D-400 epoxy in the bulk and its swollen states using a polydispersity of 1.06 are shown in *Figure 9d*. In this case, the polydispersity alone is insufficient to cause high zero angle intensity even in the bulk state (*Figure 8a*). Furthermore, the zero angle intensity of the swollen D-400 specimen is also enhanced over that of the bulk. In light of the evidence given above, the two-phase model is also preferred over the single phase model for D-400 epoxy.

The scattering from T-403 epoxy is rather similar to that from D-2000 in both the bulk and the swollen states. Although no theoretical expressions for the ideal network of T-403 epoxy are available, it is likely that T-403 epoxy structure can also best be interpreted using the two-phase model.

It is obvious that all the observed scattering behaviours can also be explained with the single phase model if sufficient amounts of both reaction defects and linkage defects are incorporated into this model. However, a theoretical expression for a defect laden network is rather difficult to derive. It is noteworthy that, even for semi-crystalline polymers, which have been studied extensively for decades, the question of single phase or two phase still remains. In terms of the two-phase model, the crystalline portion is equivalent to the ideal network part, and the amorphous phase is equivalent to the disorder part in epoxy. Regardless of the choice of models, the experimental evidence indicates that the network structures of the epoxies studied herein are rather heterogeneous.

The fraction of the molecules incorporated in the ordered network phase can be estimated using the equivalence to crystallinity in semicrystalline polymers and the general scheme of measuring crystallinity¹³. This is illustrated in *Figure 11* where two vertical lines are drawn passing through the peaks at the maxima, and the quantity $(AB + DE)/(AC + DF)$ can be regarded as an index of order in the epoxy. In order to draw an appropriate base line (line BE on *Figure 11*), knowledge of the polydispersity of the monomers is required. This is because the difference in intensity at zero angle between the experimental curve and the baseline must be consistent with the polydispersity value of the starting monomers.

Admittedly, equations (7) and (8) relating L_{ij} to $\langle r_n^2 \rangle$ are rough approximations for a network in three dimensional space. If an analytic expression for the conformation of an ideal network were available, a better match between the theory and experimental results could be expected. The Porod-Kratky approximation used in the present work is rather different from what was originally proposed. The Porod-Kratky model was originally intended to relate the contour length of a semi-rigid linear chain to $\langle r_n^2 \rangle$, the square of the distance between n segments. In the present context, we used this approximation to relate $\langle r_n^2 \rangle$ and L_{ij} where L_{ij} is not the contour length. Actually, the shortest contour length between the origin and the i, j node is far greater than L_{ij} . L_{ij} , defined as $(i^2 A^2 + j^2 A_2^2)^{1/2}$, should be regarded as the distance between the origin and the (i, j) node when the ideal network (shown in *Figure 1*) is constrained to a two dimensional space.

This approximation results in a scattering shoulder in the vicinity of 0.24 \AA^{-1} , as observed experimentally (*Figure 6*). As mentioned earlier, the peak at 0.13 \AA^{-1} originates from A_1 and the one at 0.4 \AA^{-1} corresponds to A_2 (*Figure 2a*). To a rough approximation, one can refer to the peaks at 0.13 \AA^{-1} and 0.4 \AA^{-1} as the (100) and (010) reflections. The expected strong scattering from (110) can not be the origin of the shoulder at 0.24 \AA^{-1} since the position of (110), if it exists, will be at a q value greater than 0.4 \AA^{-1} .

CONCLUSION

Prominent scattering peaks were observed in all epoxy specimens cured with three different amines. These peaks, and a portion of the total scattered intensities, can be explained in terms of an ideal network model. The intensities of neutrons scattered at zero angle from both the bulk and the swollen epoxy specimens indicate that both chemical compositions and topological connections in these epoxies are rather heterogeneous. The density fluctuation in these specimens were found to be negligible, as judged from X-ray scattering results. A two phase model accounts well for the observed phenomena, and a scheme for measuring the fraction of molecules incorporated in the ideal network is suggested.

ACKNOWLEDGEMENTS

The authors are grateful to R. J. Rubin, H. Benoit and E. A. DiMarzio for many instructive discussions. We are also indebted to C. J. Glinka, J. Gotaas, E. Prince, C. S. Choi and J. J. Rhyne for their help in the neutron

measurements, to Texaco Chemical Company for providing the amines and certain valuable technical information.

APPENDIX

Equation (12) can be deduced from equation (30) of ref. 4 by letting $\chi_{12} = \chi_{23} = \chi_{31} = 0$, where χ_{ij} is the Flory-Huggins parameter. The deuterated portion, the hydrogenated one and the solvent are denoted by components 1, 2 and 3 respectively. Alternatively, equation (12) can also be derived readily following a RPA² procedure as follows.

The Fourier transform of the concentration fluctuations $\delta\phi_i(q)$ can be related to the external perturbations $W_i(q)$ by

$$|\delta\phi_i(q)| = -\frac{1}{\kappa T} \|X_{ij}(q)\| \cdot |W_j(q) + U_j(q) + U'_j(q)| \quad (\text{A1})$$

In the present case $\|X_{ij}(q)\|$ is a 3×3 matrix and can be expressed as

$$\|X_{ij}(q)\| = \begin{vmatrix} X_1(q) & X_{12}(q) & 0 \\ X_{12}(q) & X_2(q) & 0 \\ 0 & 0 & X_3(q) \end{vmatrix} \quad (\text{A2})$$

$U_i(q)$ is the self-consistent potential and is the same for all the species. The function of $U_i(q)$ is to ensure a constant density throughout the specimen; to ascertain

$$\sum_{i=1}^3 \delta\phi_i(q) = 0.$$

$U'_j(q)$ is the other part of the self-consistent potential originated from the interactions among these three species. The interaction energy of a three component mixture can be expressed as:

$$E_{\text{mix}} = \chi_{12}\phi_1\phi_2 + \chi_{23}\phi_2\phi_3 + \chi_{31}\phi_3\phi_1 \quad (\text{A3})$$

An alternative expression for E_{mix} , whose advantage will become apparent later, is

$$E_{\text{mix}} = \frac{1}{2} [(\chi_{12} + \chi_{13} - \chi_{23})(\phi_1 - \phi_1^2) + (\chi_{23} + \chi_{21} - \chi_{31})(\phi_2 - \phi_2^2) + (\chi_{31} + \chi_{32} - \chi_{12})(\phi_3 - \phi_3^2)] \quad (\text{A4})$$

After adopting the commonly used nomenclature for a ternary system, namely $\chi_1 = \chi_{12} + \chi_{13} - \chi_{23}$ and so on, the variation of E_{mix} due to the concentration fluctuation $\delta\phi$ can be written:

$$\delta E_{\text{mix}} = -\chi_1\phi_1\delta\phi_1 - \chi_2\phi_2\delta\phi_2 - \chi_3\phi_3\delta\phi_3 \quad (\text{A5})$$

The terms linear in ϕ were neglected in the above

equation. Consequently the term $|U'_i|$ can be expressed as:

$$|U'_i(q)| = \begin{vmatrix} -\chi_1\delta\phi_1(q) \\ -\chi_2\delta\phi_2(q) \\ -\chi_3\delta\phi_3(q) \end{vmatrix} \quad (\text{A6})$$

After substituting both (A2) and (A6) into (A1) and eliminating $|U|$ through the constant density requirement, equation (A1) can be rewritten as:

$$|\delta\phi_i(q)| = -\frac{1}{\kappa T} \|X'_{ij}(q)\| |W_j(q)| \quad (\text{A7})$$

The scattered intensity for this system is

$$I(q) = |\alpha_i T| \|X'_{ij}(q)\| |\alpha_j| \quad (\text{A8})$$

More explicitly, equation (A8) can be written as:

$$I(q) = \{(\alpha_1 - \alpha_2)^2 X_x(q) + X_3(q) I_0(q) - X_3(q) X_x(q) [(\alpha_1 - \alpha_2)^2 \chi_3 + (\alpha_2 - \alpha_3)^2 \chi_1 + (\alpha_3 - \alpha_1)^2 \chi_2]\} \times \{[X_T(q) - (\chi_1 + \chi_2) X_x(q)] [1 - \chi_3 X_3(q)] + X_3(q) [1 - \chi_1 X_1(q) - \chi_2 X_2(q) + \chi_1 \chi_2 X_{12}(q)]\}^{-1} \quad (\text{A9})$$

where

$$X_x(q) = X_1(q) X_2(q) - (X_{12}(q))^2,$$

$$X_T(q) = X_1(q) + X_2(q) + 2X_{12}(q)$$

$$\text{and } I_0(q) = (\alpha_1 - \alpha_3)^2 X_1(q) + (\alpha_2 - \alpha_3)^2 X_2(q) + 2(\alpha_1 - \alpha_3)(\alpha_2 - \alpha_3) X_{12}(q)$$

By letting $\alpha_2 = \alpha_3$ and $\chi_1 = \chi_2 = \chi_3 = 0$ equation (A9) reduces to equation (12) in the main text.

REFERENCES

- 1 Wu, W. and Bauer, B. J. *Polymer* 1985, **26** (*Commun.*), 39
- 2 de Gennes, P. G. 'Scaling Concepts in Polymer Physics', Chap. X, Cornell University Press, 1979
- 3 Benoit, H. and Benmouna, M. *Macromolecules* 1984, **17**, 535
- 4 Benoit, H., Wu, W., Benmouna, M., Mozer, B., Bauer, B. and Lapp, A. *Macromolecules* 1985, **18**, 986
- 5 Morgan, R. J., Kong, F. M. and Walkup, C. M. *Polymer* 1984, **25**, 375
- 6 James, H. M. *J. Chem. Phys.* 1947, **15**(9), 651
- 7 Montroll, E. W. 'Proceedings of the Third Berkeley Symposium on Mathematical Statistics and Probability', Vol. 111, 209, Univ. of California Press, Berkeley, California, 1956
- 8 Hosemann, R. and Bagchi, S. N. 'Direct Analysis of Diffraction by Matter', North Holland, Amsterdam, 1962
- 9 Porod, G. *Monatsh. Chem.* 1949, **80**, 251
- 10 Flory, P. J. 'Statistical Mechanics of Chain Molecules', Ch. V, Interscience, 1969. (The value of l was taken from that of polyoxyethylene.)
- 11 Daoud, M. and Cotton, J. P. *J. Phys. (Paris)* 1982, **43**, 531
- 12 Tanaka, Y. and Mika, T. F. 'Epoxy Resins', Ch. 3, (Eds. C. A. May and Y. Tanaka), Decker, New York, 1973
- 13 Kakudo, M. and Kasai, N. 'X-ray Diffraction by Polymers', Ch. 13, Kodansha Ltd, 1972